

Magnetic interaction in Mg, Ti, Nb doped manganites

I.O. Troyanchuk^{1,a}, M.V. Bushinsky¹, H. Szymczak², K. Bärner³, and A. Maignan⁴

¹ Institute of Solid State and Semiconductor Physics of National Academy of Sciences, P. Brovka str. 17, 220072 Minsk, Belarus

² Institute of Physics, Polish Academy of Sciences, al. Lotnikow 32/46, 02-668 Warsaw, Poland

³ 4. Physikalisches Institut der Göttingen Universität, Bunsenstr. 13, 37073 Göttingen, Germany

⁴ Laboratoire CRISMAT, ISMRA, Université de Caen, 6 Boulevard du maréchal Juin, 14050 Caen Cedex, France

Received 24 January 2002

Published online 9 July 2002 – © EDP Sciences, Società Italiana di Fisica, Springer-Verlag 2002

Abstract. An effect of Mn substitution with Me=Mg²⁺, Ti⁴⁺, Nb⁵⁺ in manganites has been investigated by preparing La_{0.7}Sr_{0.3}(Mn_{1-x}Me_x)O₃ and La_{1-x}Sr_x(Mn_{1-x/2}Nb_{x/2})O₃ series. It was established that substitution of manganese with magnesium up to $x = 0.16$ leads to a collapse of a long-range ferromagnetic order whereas La_{0.7}Sr_{0.3}(Mn_{0.85}Nb_{0.15})O₃ is ferromagnet with $T_C = 123$ K and exhibits a large magnetoresistance below Curie point despite an absence of four-valent manganese. Hypothetical magnetic phase diagrams are constructed for La_{0.7}Sr_{0.3}(Mn_{1-x}Me_x)O₃ and La_{1-x}Sr_x(Mn_{1-x/2}Nb_{x/2})O₃. Our results show that Mn³⁺-O-Mn³⁺ exchange interaction is ferromagnetic in the orbitally disordered manganites as well as an increase of Mn⁴⁺ content above 50% from a total amount of manganese ions leads to formation of a spin glass state due to a competition between antiferromagnetic Mn⁴⁺-O-Mn⁴⁺ and ferromagnetic Mn³⁺-O-Mn⁴⁺(Mn³⁺) superexchange interactions.

PACS. 75.30.Kz Magnetic phase boundaries (including magnetic transitions, metamagnetism, etc.) – 75.30.Vn Colossal magnetoresistance – 75.30.Et Exchange and superexchange interactions

1 Introduction

La_{1-x}Sr_xMnO₃ perovskites have been of interest for many years since they exhibit anomalous magnetic and transport properties [1–6]. A discovery of colossal magnetoresistance (CMR) initiated a growing interest to manganites. In order to explain an interplay between magnetic and transport properties Zener [5] introduced a special form of exchange interactions through charge carriers – double exchange. De Gennes [7] developed a theory of double exchange and predicted that a noncollinear magnetic structure forms at intermediate concentrations between the antiferromagnetic and ferromagnetic states. The neutron diffraction data [8, 9] can be interpreted both as realization of a noncollinear magnetic structure and assuming a mixed two phase state. NMR data support the mixed phase state [10]. Further Goodenough [5] proposed arguments for the ferromagnetism to be due not only to the double exchange but also to an orbital disordering in the system of the Jahn-Teller Mn³⁺ ions. In the superexchange model, the ferromagnetic fraction of the exchange would be determined by a virtual electron transfer from half-filled e_g -orbitals of Mn³⁺ ions to empty ones. Millis [11] suggested that CMR properties of manganites in some aspects result from Jahn-Teller effect which strongly mod-

ifies the properties of Mn³⁺-containing perovskites. It is worth to be noted that there are some systems of magnetic semiconductors for example CdCr₂Se₄ [12], EuO [12] and Tl₂Mn₂O₇ [13] exhibiting CMR despite an absence of both mixed valence and Jahn-Teller effect. Since at the moment there is no general agreement on the exchange interaction mechanism in the orthomanganites as well as an origin of CMR, further studies are needed.

As it was reported in [14] La_{0.7}Sr_{0.3}(Mn_{0.7}Mn_{0.3})O₃ has a well defined critical temperature $T_C = 375$ K of the transition into ferromagnetic state. This is the highest Curie point among manganites of LaMnO₃ type. This compound exhibits a metal-like behavior of resistivity below T_C as well as a peak of magnetoresistance around T_C . Substitution of manganese with two-valent ion such as Mg²⁺ leads to increasing Mn⁴⁺/Mn³⁺ ratio and enhances the role of the interactions between Mn³⁺-Mn⁴⁺ pairs. Conversely, replacing of Mn ions with five-valent ions such as Nb⁵⁺ or Ta⁵⁺ we lower an average Mn valence and, hence, Mn³⁺-O-Mn³⁺ superexchange interaction *via* oxygen should be dominant. In this paper we report the properties of La_{0.7}Sr_{0.3}(Mn_{1-x}Me_x)O₃ (Me=Mg, Ti) as well as La_{1-x}Sr_x(Mn_{1-x/2}Nb_{x/2})O₂ series. Our results indicate an important role of superexchange ferromagnetic interactions in the manganites.

^a e-mail: troyan@ifitp.bas-net.by

Table 1. Unit cell parameters (a , b , c , α , V), and Mn^{4+} content calculated for some compositions.

Composition	a (Å)	b (Å)	c (Å)	α (deg.)	V (Å ³)	% Mn^{4+}	T_f , T_c (K)
$\text{La}_{0.8}\text{Sr}_{0.2}(\text{Mn}_{0.9}\text{Nb}_{0.1})\text{O}_3$	5.558	5.579	7.858	–	243.675	0	120
$\text{La}_{0.7}\text{Sr}_{0.3}(\text{Mn}_{0.85}\text{Nb}_{0.15})\text{O}_3$	5.560	5.580	7.859	–	243.790	0	123
$\text{La}_{0.5}\text{Sr}_{0.5}(\text{Mn}_{0.75}\text{Nb}_{0.25})\text{O}_3$	5.579	5.593	7.867	–	245.477	0	30
$\text{La}_{0.7}\text{Sr}_{0.3}(\text{Mn}_{0.85}\text{Mg}_{0.15})\text{O}_3$	3.878	–	–	90.36	58.2999	45	72
$\text{La}_{0.7}\text{Sr}_{0.3}(\text{Mn}_{0.7}\text{Ti}_{0.3})\text{O}_3$	3.911	–	–	90.42	58.815	0	80

2 Experimental

Polycrystalline samples were prepared from high purity carbonate SrCO_3 and oxides La_2O_3 , MnO_2 , TiO_2 , Nb_2O_5 or MgO mixed in stoichiometric ratio using conventional ceramic technology. Pellets were pre-fired at 1000 °C, then ground, pressed and synthesized at 1550 °C in air, then cooled down room temperature at a rate of 150 °C/h. A well textured $\text{La}_{0.7}\text{Sr}_{0.3}(\text{Mn}_{0.85}\text{Nb}_{0.15})\text{O}_3$ sample was prepared using the floating zone method. In order to minimize a possible content of Mn^{4+} ions the $\text{La}_{1-x}\text{Sr}_x(\text{Mn}_{1-x/2}\text{Nb}_{x/2})\text{O}_3$ samples were annealed at 800 °C during 24 h in evacuated quartz tubes. Oxygen content has been checked by thermogravimetric analysis (TGA). According to X-ray data all the samples were single phase. Magnetization was measured with a Foner vibrating sample magnetometer. Resistivity measurements were performed by a standard four probes method. Contacts were formed using ultrasonically deposited indium.

3 Results and discussion

TGA performed in hydrogen medium has shown the oxygen content to be very close to the stoichiometric one. The X-ray patterns show the rhombohedral unit cell for both $\text{La}_{0.7}\text{Sr}_{0.3}(\text{Mn}_{1-x}\text{Ti}_x)\text{O}_3$ and $\text{La}_{0.7}\text{Sr}_{0.3}(\text{Mn}_{1-x}\text{Mg}_x)\text{O}_3$ compositions (Tab. 1). The structure of $\text{La}_{1-x}\text{Sr}_x(\text{Mn}_{1-x/2}\text{Nb}_{x/2})\text{O}_3$ series is O^{I} -orthorhombic ($c\sqrt{2} < a < b$) at $x \leq 0.1$ and O -orthorhombic ($a < c\sqrt{2} < b$) for $x \geq 0.2$. LaMnO_3 is known to exhibit a cooperative Jahn-Teller orbital ordering which vanishes at $T_{JT} = 750$ K [15]. The orbital ordering leads to a strong enhancement of crystal structure distortions. According to Goodenough's consideration [16,17] O^{I} -crystal distortion may indicate an orbital ordering. The small O -orthorhombic distortions revealed in $x \geq 0.2$ compositions are incompatible with the orbital ordering. It is worth to be noted that unit cell parameters of $\text{La}_{0.7}\text{Sr}_{0.3}(\text{Mn}_{0.85}\text{Mg}_{0.15})\text{O}_3$ are less than those of $\text{La}_{0.7}\text{Sr}_{0.3}(\text{Mn}_{0.85}\text{Nb}_{0.15})\text{O}_3$ in spite of a fact that Mg^{2+} ionic radius (0.88 Å for six-fold coordination) is larger than for Nb^{5+} (0.78 Å). Such a behavior results from a conversion of Mn^{3+} into Mn^{4+} in the Mg^{2+} doped samples. According to [18] Mn^{4+} ionic radius is 0.67 Å whereas for Mn^{3+} it is much larger – 0.78 Å. In Table 1 the Mn^{4+} ions content is accounted by suggesting the samples to be stoichiometric in agreement with TGA data.

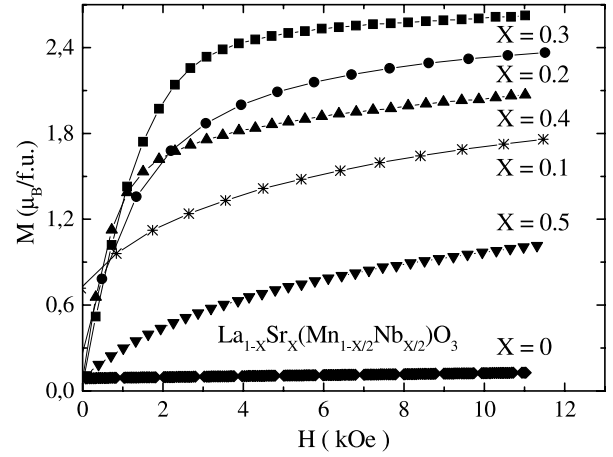
**Fig. 1.** Magnetization *vs.* field for $\text{La}_{1-x}\text{Sr}_x(\text{Mn}_{1-x/2}\text{Nb}_{x/2})\text{O}_3$ at 5 K.

Figure 1 shows the magnetization *vs.* magnetic field at 5 K for $\text{La}_{1-x}\text{Sr}_x(\text{Mn}_{1-x/2}\text{Nb}_{x/2})\text{O}_3$ series. The parent LaMnO_3 compound shows the spontaneous magnetization value at 5 K corresponding to magnetic moment of 0.07 μ_B per Mn^{3+} ion. The Néel point where spontaneous magnetization develops is 143 K. According to [19] the spontaneous magnetization has a relativistic nature. Substitution of Mn with Nb leads to an enhancement of the spontaneous magnetization whereas the temperature of transition into paramagnetic state slightly decreases (Figs. 1 and 2). In accordance with the magnetization data the $\text{La}_{0.8}\text{Sr}_{0.2}(\text{Mn}_{0.9}\text{Nb}_{0.1})\text{O}_3$ and $\text{La}_{0.7}\text{Sr}_{0.3}(\text{Mn}_{0.85}\text{Nb}_{0.15})\text{O}_3$ samples are ferromagnets with the magnetic moment per chemical formula around 2.3 μ_B and 2.6 μ_B respectively. Neutron diffraction study has revealed the magnetic moment of Mn^{3+} in the parent LaMnO_3 antiferromagnetic compound to be close to 3.5 μ_B [8] whereas Nb^{5+} is diamagnetic ion, hence the expected moment should be close to 3 μ_B per formula unit what is in a rather good agreement with the observed one. The Nb doped sample ($x = 0.3$) has a well defined Curie point – 123 K as it is clearly seen from the magnetization *vs.* temperature dependence in low magnetic field (Fig. 2). It is interesting to note that our sample $\text{La}_{0.7}\text{Sr}_{0.3}(\text{Mn}_{0.85}\text{Ta}_{0.15})\text{O}_3$ containing Ta instead Nb has a very close $T_C = 124$ K. Both Curie point and spontaneous magnetization start gradually to decrease when Nb content exceeds 15% from total sites number in the

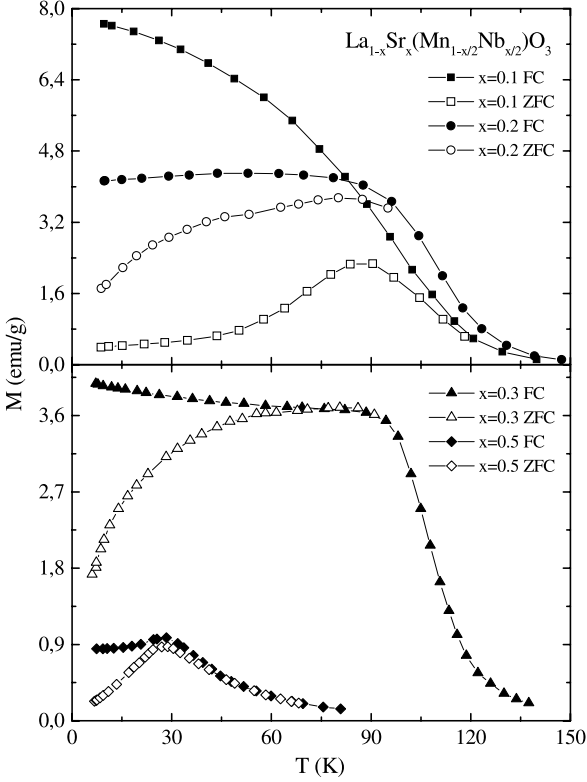


Fig. 2. ZFC and FC magnetizations *vs.* temperature dependencies for Nb-substituted compositions ($x = 0.1, 0.2$ – upper panel; $0.3, 0.5$ – lower panel).

manganese sublattice. The difference between ZFC and FC magnetizations becomes more pronounced below 30 K. The magnetic state cardinally changes as the concentration of niobium reaches 25%. We have observed the magnetic susceptibility of the $x = 0.5$ sample dramatically decreases. ZFC-magnetization shows a peak at 30 K. Below this temperature FC magnetization practically does not change. Taking into account the character of $M(H)$ dependence (Fig. 1) we have concluded that the sample $x = 0.5$ can be considered as spin glass with $T_f = 30$ K.

According to resistivity *vs.* temperature measurements (Fig. 3) $\text{La}_{0.7}\text{Sr}_{0.3}(\text{Mn}_{0.85}\text{Nb}_{0.15})\text{O}_3$ is semiconductor. The resistivity at $T = 77$ K is very large – around 10^7 Ohm cm. Below Curie point we observed a large magnetoresistance defined as $\{[\rho(H = 9 \text{ kOe}) - \rho(H = 0)]/\rho(H = 0)\} \times 100\%$. The magnitude of magnetoresistance (25% in a field of 9 kOe) is comparable with that for mixed valence manganites around Curie point.

Hypothetical magnetic phase diagram of $\text{La}_{1-x}\text{Sr}_x(\text{Mn}_{1-x/2}\text{Nb}_{x/2})\text{O}_3$ is shown in Figure 4. We believe that the concentration transition from antiferromagnetic ($x = 0$) to ferromagnetic state takes place through a mixed two phase state. Really the both magnetic properties $M(H)$ and $M(T)$ for $\text{La}_{0.9}\text{Sr}_{0.1}\text{Mn}_{0.95}\text{Nb}_{0.05}\text{O}_3$ composition strongly resemble those for lightly Ca or Sr doped manganites [20]. According to NMR [10] and neutron diffraction data [8,9] for lightly doped manganites two phase magnetic state

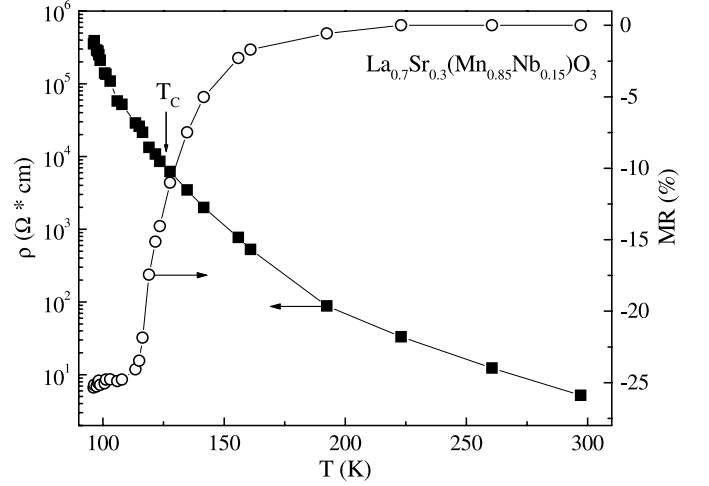


Fig. 3. Resistivity and MR for $\text{La}_{0.7}\text{Sr}_{0.3}(\text{Mn}_{0.85}\text{Nb}_{0.15})\text{O}_3$.

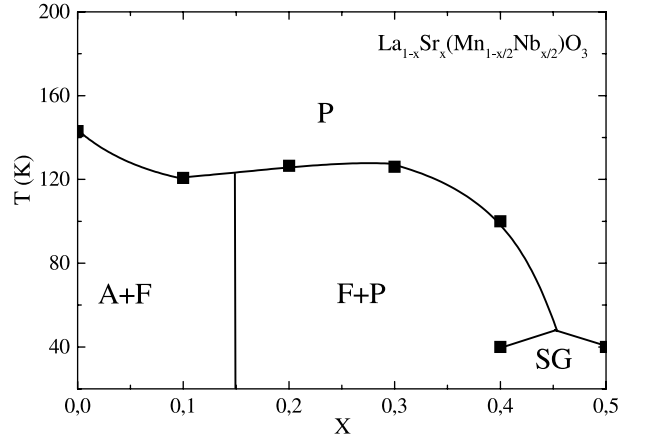


Fig. 4. Magnetic phase diagram for $\text{La}_{1-x}\text{Sr}_x(\text{Mn}_{1-x/2}\text{Nb}_{x/2})\text{O}_3$ series (A – antiferromagnet; F – ferromagnet; P – paramagnet; SG – spin glass).

is much more probable than a canted one. For the ferromagnetic compositions $0.2 \leq x \leq 0.4$ a small part of manganese ions seems to be paramagnetic due to a break of magnetic interactions in domains enriched with diamagnetic Nb^{5+} ions. Around $x = 0.25$ Nb-concentration the long range ferromagnetic order collapses due to a diamagnetic dilution of Mn-sublattice.

Manganese substitution with titanium in $\text{La}_{0.7}\text{Sr}_{0.3}(\text{Mn}_{1-y}\text{Ti}_y)\text{O}_3$ series leads to gradual decreasing both magnetization and Curie point. ZFC and FC magnetizations behavior for strongly doped samples is displayed in Figure 5. Contrary to a parent non-substituted compound $\text{La}_{0.7}\text{Sr}_{0.3}(\text{Mn}_{0.8}\text{Ti}_{0.2})\text{O}_3$ exhibits a broad transition into paramagnetic state which starts at $T = 120$ K and finishes at $T = 170$ K. By analyzing $M(T)$ and $M(H)$ (Figs. 5, 6) curves we have concluded that the $y = 0.3$ composition has a strongly pronounced spin-glass component. However, the long range order seems to be preserved for this sample. The hypothetical magnetic phase diagram obtained on the base of magnetization data is shown in Figure 8 (upper panel).

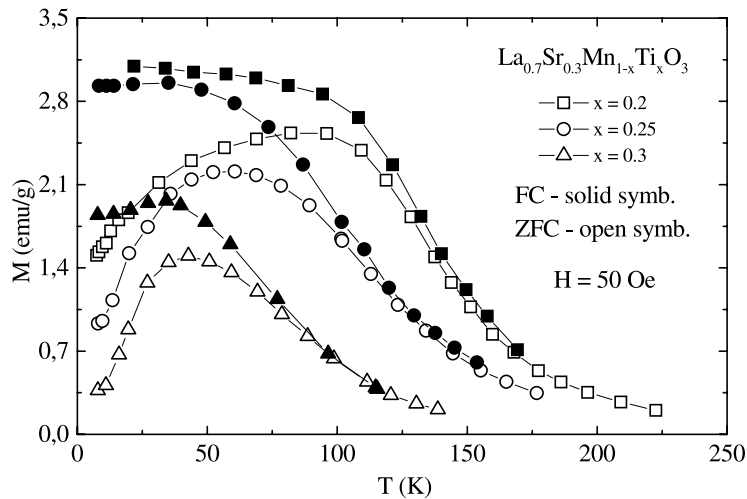


Fig. 5. ZFC and FC magnetizations for $\text{La}_{0.7}\text{Sr}_{0.3}(\text{Mn}_{1-x}\text{Ti}_x)\text{O}_3$ series.

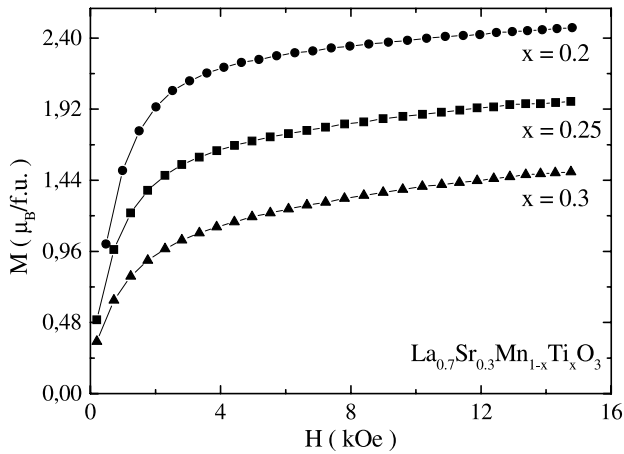


Fig. 6. Magnetization *vs.* field for titanium-substituted manganites.

The sample doped by Mg^{2+} ($y = 0.08$) shows the magnetization value expected for the ferromagnetic state whereas small magnetic moments observed for $x = 0.15$ and $x = 0.20$ compositions are incompatible with ferromagnetic ground state. Strong dependence of magnetization on magnetic field in fields above 5 kOe could be attributed to a non-homogenous magnetic state. Results of study of ac-magnetic susceptibility for the $y = 0.15$ sample are presented in Figure 7. Real part of susceptibility shows a peak around 47 K. Increasing frequency of an external field from 1 to 100 Hz weakly affects the data. Imaginary part of the magnetic susceptibility exhibits an anomalous behavior around 40 K, 70 K and 140 K. The data depend on frequency below 140 K. Positions of the peaks at both 40 K and 70 K shift forward to high temperature with increasing frequency. We think that the sample at high temperature contains large ferromagnetic clusters which start to freeze below 140 K. Around 70 K the long-range ferro-

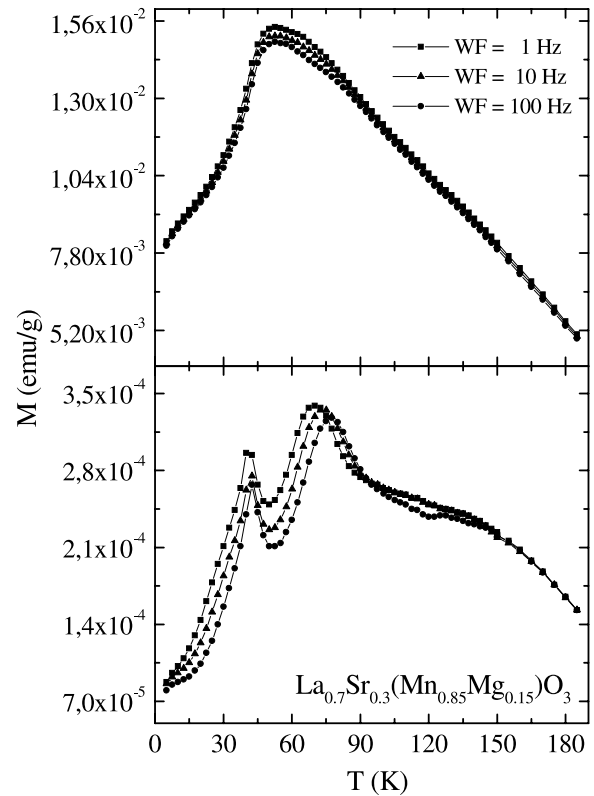


Fig. 7. Real (upper panel) and imagined (lower panel) parts of magnetic susceptibility for $\text{La}_{0.7}\text{Sr}_{0.3}(\text{Mn}_{0.85}\text{Mg}_{0.15})\text{O}_3$ sample.

magnetic order seems to appear, whereas at 40 K the spin glass-like state develops due to a competition between ferromagnetic and antiferromagnetic exchange interactions.

For the Mg ($y = 0.20$) sample we have observed $M(H)$ and $M(T)$ dependencies typical for the spin glass. Apparently the long range magnetic order is collapsed in this

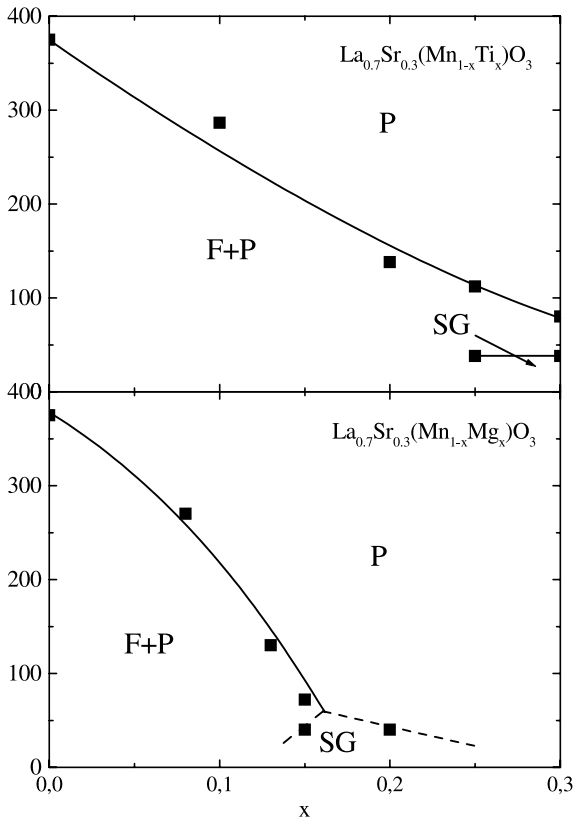


Fig. 8. Magnetic phase diagrams for $\text{La}_{0.7}\text{Sr}_{0.3}(\text{Mn}_{1-x}\text{Ti}_x)\text{O}_3$ (upper panel) and $\text{La}_{0.7}\text{Sr}_{0.3}(\text{Mn}_{1-x}\text{Mg}_x)\text{O}_3$ (lower panel) series.

sample. The magnetic phase diagram is presented in Figure 8 (lower panel).

The results presented here deal with the facts that the $\text{La}_{0.7}\text{Sr}_{0.3}(\text{Mn}_{0.85}^{3+}\text{Nb}_{0.15}^{5+})\text{O}_3$ samples enriched with Mn^{3+} ions are ferromagnetic and show a large magnetoresistance whereas the $\text{La}_{0.7}\text{Sr}_{0.3}(\text{Mn}_{0.45}^{4+}\text{Mn}_{0.3}^{3+}\text{Mg}_{0.15}^{2+})\text{O}_3$ samples with Mn^{4+} content above 50% from a total content of manganese ions become spin glasses. This result indicates an important role of ferromagnetic superexchange *via* oxygen scenario of magnetic interactions in manganites. According to the superexchange mechanism the $\text{Mn}^{3+}\text{-O-Mn}^{3+}$ and $\text{Mn}^{3+}\text{-O-Mn}^{4+}$ 180° magnetic interactions are strongly ferromagnetic for the orbitally disordered state whereas the $\text{Mn}^{4+}\text{-O-Mn}^{4+}$ ones are strongly antiferromagnetic [6]. The Curie point associated with $\text{Mn}^{3+}\text{-O-Mn}^{3+}$ positive superexchange may be close to room temperature for manganites with perovskite structure because our samples contain diamagnetic Nb^{5+} ions which should strongly decrease Curie point. Stoichiometric $\text{LaMn}^{3+}\text{O}_3$ compound also shows ferromagnetic interactions between Mn^{3+} ions when cooperative Jahn-Teller distortions are vanished at $T = 750$ K [5]. According to Goodenough's consideration the orbital ordering changes character of superexchange magnetic interactions which in the orbitally ordered state become anisotropic [16,17].

Taking into account the ferromagnetic character of $\text{Mn}^{3+}\text{-O-Mn}^{3+}$ exchange interactions we can explain the

asymmetry in properties for the hole- and electron-doped manganites. The electron-doped manganites are as a rule charge ordered antiferromagnets, whereas the hole-doped ones exhibit the ferromagnetic or spin glass behavior depending on rare-earth ionic radii [21]. According to the superexchange model such a type of behavior results from a role of $\text{Mn}^{4+}\text{-O-Mn}^{4+}$ antiferromagnetic interactions more important in comparison with $\text{Mn}^{3+}\text{-O-Mn}^{3+}$ and $\text{Mn}^{3+}\text{-O-Mn}^{4+}$ ones while a concentration of Mn^{4+} species increases. The $\text{Mn}^{3+}\text{-O-Mn}^{3+}$ magnetic interaction strongly depends on Mn-O-Mn angle value. Decrease of Mn-O-Mn angle reduces the ferromagnetic part of exchange interactions.

We suggest an electrical conductivity of $\text{La}_{1-x}\text{Sr}_x(\text{Mn}_{1-x/2}^{3+}\text{Nb}_{x/2}^{5+})\text{O}_3$ series to be associated with small amount of Mn^{4+} or Mn^{2+} ions which appears as result of small deviation from oxygen stoichiometry or nonhomogeneous distribution of manganese and niobium ions. It is likely that these ions create shallow acceptor levels near wide oxygen valence band. A concentration of these impurities is too small to create an impurity band expected for the samples enriched with Mn^{4+} ions. An external magnetic field may strongly reduce a binding energy for such trapped states due to a polarization of manganese magnetic moments when magnetic ordering starts to develop. On the other hand the magnetoresistance in the polycrystalline samples is dominated by transport across grain boundaries. In such a case the magnetoresistance increases gradually as temperature decreases [22]. However, we have observed nonmonotonic behavior of magnetoresistance dependence *vs.* temperature (Fig. 3). So we assume the magnetoresistance to result from both intrinsic effect near T_C and spin-polarized electrical transport between grains.

This work was supported by Polish Committee for Scientific research (KBN grant 5 P03B 016 20) and Belarus Fund for Fundamental Research (Grant F01-039).

References

1. J. Van Santen, G.H. Jonker, *Physica* **16**, 599 (1950)
2. B. Raveau, A. Maignan, V. Caignaert, *J. Solid State Chem.* **117**, 424 (1995)
3. Y. Tomioka, A. Asamitsu, H. Kuwahara, Y. Tokura, *Phys. Rev.* **53**, R1689 (1996)
4. M.R. Ibarra, P.A. Algarabel, C. Marquina, J. Blasco, J. Garcia, *Phys. Rev. Lett.* **75**, 3541 (1995)
5. C. Zener, *Phys. Rev.* **82**, 403 (1955)
6. J.B. Goodenough, *Magnetism and the Chemical Bond* (Interscience, New-York/London 1963)
7. P.G. de Gennes, *Phys. Rev.* **118**, 141 (1960)
8. E.O. Wollan, W.C. Koehler, *Phys. Rev.* **100**, 545 (1955)
9. Z. Jirak, S. Vratilav, J. Zajicek, *Phys. Status Solidi (a)* **52**, 39 (1979)

10. G. Allodi, R. De Renzi, G. Guidi, F. Licci, M.W. Pieper, Phys. Rev. B **56**, 6036 (1997)
11. A.J. Millis, P.B. Littlewood, B.I. Shraiman, Phys. Rev. Lett. **74**, 5144 (1995)
12. S. Methfessel, D.C. Mattis, *Magnetic Semiconductors. Handbuch der Physik, XVIII/1* (Springer, Berlin, 1968)
13. J.A. Alonso, M.J. Martínez-Lope, M.T. Casais, P. Velasco, J.L. Martínez, M.T. Fernández-Díaz, J.M. de Paoli, Phys. Rev. B **60**, R15 024 (1999)
14. A. Urushibara, Y. Moritomo, T. Arima, A. Asamitsu, G. Kido, Y. Tokura, Phys. Rev. B **51**, 41103 (1995)
15. J. Rodríguez-Carvajal, M. Hennion, F. Moussa, A.H. Moudden, L. Pinsard, A. Revcolevschi, Phys. Rev. B **57**, R3189 (1998)
16. J.B. Goodenough, A. Wold, R.J. Arnott, N. Menyuk, Phys. Rev. **124**, 373 (1961)
17. J.S. Zhou, J.B. Goodenough, Phys. Rev. B **60**, R15002 (1999)
18. R.D. Shannon, Acta Cryst. Sect. A **32**, 751 (1976)
19. Robert L. Rasera, Gary L. Catchen, Phys. Rev. B **58**, 3218 (1998)
20. F. Moussa, M. Hennion, G. Biotteau, J. Rodríguez-Carvajal, L. Pinsard, A. Revcolevschi, Phys. Rev. B **60**, 12299 (1999)
21. M. Hervieu, A. Barnabé, C. Martin, A. Maignan, F. Damay, B. Raveau, Eur. Phys. J. B **8**, 31 (1999)
22. H.Y. Hwang, S.W. Cheong, N.P. Ong, B. Batlogg, Phys. Rev. Lett. **77**, 2041 (1996)